TRENDS IN SCIENCES 2026; 23(12): 13914
https://doi.org/10.48048/tis.2026.13914
RESEARCH ARTICLE

Biodegradable Bioplastics Synthesized from BSFL Pupae Chitosan and OPEFB Cellulose: Influence of Citric Acid on Material Properties

Novianti Adi Rohmanna[1,*], Utami Irawati[2], Muhammad Rido[3], Hemy Sriana[4], Muhammad Rasad[1] and Fidel Castro Haholongan Purba[1]

[1]*Department of Agroindustrial Technology, Faculty of Agriculture, Lambung Mangkurat University, Banjarbaru, Indonesia*
[2]*Department of Chemistry, Faculty of Mathematics and Natural Sciences, Lambung Mangkurat University, Banjarbaru, Indonesia*
[3]*Department of Animal Science, Faculty of Agriculture, Lambung Mangkurat University, Banjarbaru, Indonesia*
[4]*Department of Agronomy, Faculty of Agriculture, Lambung Mangkurat University, Banjarbaru, Indonesia*

([*]Corresponding author's e-mail: novianti.rohmanna@ulm.ac.id)

Received: 26 March 2026, Revised: 17 May 2026, Accepted: 24 May 2026, Published: 10 July 2026

Abstract

The development of biodegradable plastics from renewable resources has gained increasing attention as a strategy to reduce dependence on petroleum-based materials. In this study, bioplastics were prepared using chitosan derived from black soldier fly (BSF, *Hermetia illucens*) pupae and cellulose extracted from oil palm empty fruit bunches (OPEFB), with citric acid (CA) incorporated as a network-modifying agent. The objective of this work was to evaluate the influence of citric acid concentration on the structural, mechanical, physical, and biodegradation properties of the resulting bioplastic films. Bioplastics were synthesized from BSF-derived chitosan (1.5% (w/v)), starch (3% (w/v)), and OPEFB cellulose (0.06 g), with CA added at concentrations ranging from 0 to 10 wt% relative to total polymer content. The results showed that CA addition significantly influenced film performance ($p > 0.05$). The tensile strength increased significantly from 0.13 to 0.64 MPa at 2.5 wt% CA, indicating improved intermolecular interactions within the polymer matrix. In contrast, elongation at break decreased with increasing CA concentration, suggesting reduced polymer chain mobility. Physical characterization revealed that the incorporation of CA reduced moisture content and swelling degree, with the lowest values observed at 2.5 wt% CA. FTIR analysis indicated that hydrogen-bond-mediated interaction contributed significantly to the polymer network, although direct quantitative confirmation of the dominant interaction mechanism was not performed. Morphological observations confirmed that moderate CA addition produced a more compact and homogeneous structure, whereas excessive CA resulted in surface irregularities. Biodegradation tests further demonstrated that citric acid affected degradation behavior by altering polymer network density and hydrophilicity. Overall, the results suggest that controlled addition of citric acid plays an important role in tailoring the properties of bioplastics derived from BSF pupae chitosan and OPEFB cellulose, highlighting the potential of integrating insect biomass and agricultural residues for sustainable bioplastic production.

Keywords: Bioplastic, Black soldier fly larvae, Chitosan pupae, Cellulose OPEFB, Citric acid, Polymer, Hydrogen-bonding

Introduction

Plastic has become a mainstay of modern life due to its lightweight, durable, and flexible properties [1]. Commercial plastics are produced from petroleum-derived materials, such as polyethylene (PE), polypropylene (PP), and polystyrene (PS). However, these materials exhibit high resistance to natural

degradation, allowing them to persist in the environment for hundreds of years without decomposing, thereby increasing environmental pollution [2]. In addition, the degradation of conventional plastic can generate microplastics that may threaten environmental and health risks [1]. These concerns have intensified interest in the development of environmentally friendly alternatives such asbioplastic.

Bioplastics [3-5] are commonly derived from renewable biological resources such as starch [2], cellulose [2], chitosan [3], and proteins [6]. In recent years, the demand for bioplastics has increased substantially [7]; however, their production has been predominantly reliant on food-based feedstocks, including tapioca [8], cassava [9], and potato [10]. This dependence raises environmental and agricultural concerns, particularly related to competition with food resources and the long-term sustainability of bioplastic production systems. To address these challenges, the utilization of non-food biomass as raw materials for bioplastic production has gained increasing attention. Agricultural residues and insect-derived waste represent abundant, low-cost, and renewable resources that align with circular economy principles. Nevertheless, the application of insect-based and agricultural waste-derived biopolymers for bioplastic development remains limited and insufficiently explored. Therefore, investigating alternative, waste-based biopolymer sources is essential to support sustainable agricultural practices and environmentally responsible material development.

The Black Soldier Fly (BSF, *Hermetia illucens*) is an insect widely recognized for its ability to bioconvert organic waste into valuable insect biomass [11,12], including pupae as one of its life stages [13-15]. BSF pupae contain approximately 35% chitin [13], making them a promising and novel source of chitosan [14,16]. Chitosan is a functional biopolymer that has been extensively studied for its potential to enhance the performance of bioplastics [3]. However, chitosan derived from BSF exhibits distinct characteristics compared to commercial chitosan, particularly in terms of molecular weight and degree of deacetylation [17]. These differences significantly influence polymer–polymer interactions, mechanical behavior, and the degradation performance of the resulting bioplastics [18]. Ianniciello *et al.* [19] reported that films produced solely from BSF-derived chitosan tend to exhibit relatively low tensile strength and elasticity. Therefore, material modification or reinforcement strategies, such as the incorporation of cellulose, are necessary to improve the overall properties of BSF-based bioplastics. Cellulose is a natural polysaccharide composed of long chains of glucose units linked by β-1,4-glycosidic bonds [20] and widely used as a reinforcing agent in bioplastic systems due to its high stiffness and mechanical strength. In particular, cellulose extracted from oil palm empty fruit bunches (OPEFB), an abundant agro-industrial residue, represents an attractive reinforcement material [21]. Previous studies reported that OPEFB consists of approximately 44% - 66% cellulose, 18% - 32% hemicellulose, and 14% - 36% lignin, highlighting its potential as a biomass for bio-based material applications [22].

Recent studies have explored various biodegradable polymers, particularly chitosan and cellulose, for sustainable bioplastic production. Nevertheless, most previous studies have focused on crustacean-derived chitosan, which remains dependent on seasonal marine waste resources and may raise allergen-related concerns. In contrast, chitosan derived from BSF pupae represents a promising alternative due to its sustainable biomass availability, rapid production cycle, and potential for circular bioeconomy applications. Despite this potential, the utilization of BSF-derived Chitosan in combination with OPEFB Cellulose for bioplastic applications remains limited. This study focuses on understanding the structure-property relationships of bioplastics formulated from BSF-derived chitosan and OPEFB cellulose. Citric acid (CA) is introduced as a network-modifying agent to promote intermolecular interactions [6,23-25], primarily through hydrogen bonding, and to improve polymer cohesion within the bioplastic matrix [5,8]. This approach is particularly relevant for the development of bioplastics with reduced water sensitivity, permeability, and component migration [25], while emphasizing environmental sustainability and functional tensile performance rather than high load-bearing capacity. Currently, studies exploring bioplastics derived from BSF pupae-based chitosan reinforced with OPEFB-based cellulose remain limited. Moreover, the influence of citric acid on the structural, physical, and mechanical properties of such waste-based

bioplastic systems has not been sufficiently elucidated. Therefore, this study investigates the effect of citric acid addition (0, 2.5, 7.5 and 10 wt%) based on total polymer content) on the bioplastic properties. Chitosan-based bioplastics and citric-acid-modified polysaccharide films have been widely studied due to their biodegradability and potential for sustainable packaging applications. Previous studies have shown that citric acid can improve the mechanical properties, structural cohesion, and water resistance of polysaccharide-based films by promoting intermolecular interactions within the polymer matrix [10,23,24]. At the same time, black soldier fly (BSF) biomass has gained increasing attention as an alternative and sustainable source of chitosan, offering advantages in terms of availability and waste valorization [17,2]. In addition, cellulose derived from oil palm empty fruit bunches (OPEFB) has been reported to function effectively as a reinforcing component, contributing to improved structural stability and mechanical performance in biopolymer systems [5,21]. Despite these advances, the use of chitosan derived specifically from BSF pupae in combination with OPEFB-derived cellulose for bioplastic production has received limited attention. Furthermore, the role of citric acid in influencing the structural characteristics and resulting physical, mechanical, and biodegradation behavior of such waste-derived polymer systems remains insufficiently understood. Therefore, this study investigates the effect of citric acid concentration on the structural, mechanical, physical, and biodegradation properties of bioplastics prepared from BSF pupae-derived chitosan reinforced with OPEFB-derived cellulose.

Materials and methods

Preparation of the BSF sample

In this study, pupae shells were collected from single local breeder, where BSFL larvae were fed food waste before developing into pupae. Before and during transport to the laboratory, the sample was sealed in plastic bags and stored at room temperature. BSFL were cleaned and weighed, and then dried in an oven for 24 h at 65 °C. The sample was ground using a grinder and then sifted through a 35-mesh screen. The sample was then saved for proximate analysis and chitosan extraction.

Extraction of chitosan

The chitosan extraction was modified from El Feky *et al.* [26]. Approximately 100 g of ground pupae, respectively, were treated with n-hexane (1:5 (w/v)) for 24 h at room temperature to remove lipids. After 24 h, the solution was removed from the sample, which was then dried in an oven at 65 °C for 2 h. The sample was deproteinized with 1 M NaOH (1:10 (w/v)) for 2 h at 80 °C, and it was stirred with a magnetic stirrer to remove the protein. The sample was then washed with distilled water, repeatedly rinsed until the pH became neutral, and subsequently dried in an oven at 65 °C for 24 h. The sample was demineralized by 1 M HCl (1:10 (w/v)) at 95 °C for 1 h to produce chitin. Chitin was then washed with distilled water, repeatedly rinsed until the pH became neutral, and subsequently dried in an oven at 65 °C for 24 h. Chitin was then treated with 3% H_2O_2 (1:10 (w/v)) for 3 h at 90 °C, using a magnetic stirrer to decolorize it further. During the process, the pH is adjusted to 10 to optimize H_2O_2. The sample is then washed with distilled water until the pH reaches neutral. The chitin was then dried in an oven at 65 °C for 24 h. To synthesize chitosan, the last process involves treating chitin with 40% NaOH (1:10 (w/v)) for 3 h at 90 °C. The sample was washed with distilled water to remove the alkali until the pH reached a neutral level. The chitosan was then dried in an oven at 65 °C for 24 h. After extraction, the chitosan was ground and stored in airtight containers in a desiccator at room temperature to prevent moisture absorption prior to characterization and bioplastic preparation.

Depigmentation of cellulose OPEFB

The unbleached cellulose from Empty fruit bunch (EFB) was collected from PT CPKA in Pelaihari, South Kalimantan, Indonesia. The unbleached cellulose was treated with 3% H_2O_2 (1:20 (w/v)) for 3 h at 90 °C (pH adjusted to 10), using a magnetic stirrer to decolorize it further. To remove H_2O_2, the sample was washed with distilled water, repeatedly rinsed until the pH became neutral, and then dried in an oven at 60 °C for 24 h.

Bioplastic synthesis

Bioplastic synthesis modified from Khadsai *et al.* [24]. Chitosan from pupae (CS, 1.5% (w/v)) was dissolved in 1% w/w glacial acetic acid and stirred at 75 °C for 50 min. The starch (tapioca flour) (S, 3% (w/v))

and 0.06 g of cellulose were dissolved in distilled water and stirred on a hot plate at 70 °C for 40 min. For composite film preparation, 3 mL of glycerol was added, and the mixture was magnetically stirred at 70 °C for 30 min approximately 500 rpm to ensure homogeneous mixing. The blended chitosan/cellulose/starch (CS/C/S) bioplastic was prepared at a 1:1 (w/w) ratio. Thereafter, citric acid (CA, % (w/w)) (based on the total weight of CS, C, and S) was added to the CS/C/S solution, together with NaH_2PO_4 (50% (w/w), based on the total weight of CA) as the catalyst of the reaction. The solution was further mixed for 30 min. Afterward, approximately 40 mL of bioplastic solution is poured into the strangle mold casts and then dried overnight at 60 °C in an oven to obtain the films. All the films were conditioned in a desiccator and left for 48 h before analysis. A base for formulating the bioplastic composition, as shown in **Table 1**. Each formulation was prepared independently, and all characterizations and mechanical testing was performed in five replicates. The experimental design was intended to ensure reproducibility and enable statistical comparison of material properties.

Table 1 A base for the formulation of bioplastic composition.

Bioplastic types	Composition					
	Chitosan (CS) (% (w/v))	**Cellulose (C) (g)**	**Glycerol (mL)**	**Starch (S) (% (w/v))**	**Citric acid (% (w/w))**	**NaH_2PO_4 (% (w/w))**
CS/C/S	1.5	0.06	3	3	-	-
CS/C/S/2,5CA	1.5	0.06	3	3	2.5	50
CS/C/S/5CA	1.5	0.06	3	3	5	50
CS/C/S/7,5CA	1.5	0.06	3	3	7.5	50
CS/C/S/10CA	1.5	0.06	3	3	10	50

Chitosan characterization

Chitosan Yield (CY)

The chitosan yield was calculated to evaluate the effectiveness of the extraction process from BSF pupae. This parameter reflects the amount of chitosan successfully recovered relative to the initial dry weight of the raw material. The yield was determined using the following equation:

$$\text{yield } (\%) = \frac{W_1}{W_0} \times 100 \quad (1)$$

where W_1 is the dry weight of the extracted chitosan (g), and W_0 is the initial dry weight of the BSF pupae powder used for extraction (g). All measurements were performed in triplicate, and the results are reported as mean ± standard deviation.

Degree of Deacetylation (DD%)

The acid-base titration method was adapted by El Feky *et al.* [26] to determine the degree of deacetylation (DD) of the derived chitosan. Briefly, 0.125 g of chitosan was weighed and mixed with 30 mL of 0.1 M HCl, then approximately 5 drops of methyl orange were added as an indicator. The mixture was stirred for 30 min at room temperature until it became homogeneous. It was then titrated with 0.1 M NaOH until the red chitosan solution turned orange. Using Eq. (2), the DD% of chitosan was determined.

$$\text{DD\%} = \frac{C1V1 - C2V2}{M \times 0.0994} \times 0.016 \times 100 \quad (2)$$

where C1 and C2 are concentrations of HCl and NaOH (mol/L), V1 is the volume of 0.1 M HCl (mL), V2 is the volume of 0.1 M NaOH (mL), and M is the weight of chitosan (g). The mass of the NH_2 group in 1 mL of 1 M standard HCl, expressed in grams, serves as a reference factor in Eq. (1). The corresponding weight ratio of NH_2 groups in the resulting chitosan is 0.099433.

Solubility of chitosan

The filter paper was weighed before and after filtration. Approximately 1 g of chitosan was dissolved in 99 mL of distilled water containing 1% glacial acetic acid using a magnetic stirrer for 30 min. The sample was extracted, the residue was filtered through Whatman No. 1 filter paper, and the residue was weighed [26].

Cellulose characterization

Fourier-Transform Infrared (FTIR) spectroscopy

FTIR in attenuated total reflection (ATR) mode, utilizing 32 scans at a resolution of 4 cm^{-1} within the wavenumber range of 4,000 to 600 cm^{-1} to characterize the functional groups on the material surfaces.

X-Ray Diffraction (XRD)

X-ray powder diffraction (XRPD) patterns were obtained using a AXS D8 ADVANCE diffractometer (Bruker, Billerica, MA, USA) in reflection mode with Bragg-Brentano geometry, using an interval of 5° - 40° (2θ), operating with a radiation source of monochromatic X-rays at Cu Kα (λ = 1.5406 Å), using a LYNXEYE_XE_T detector, and applying 40 kV and 40 mA as the voltage and amperage, respectively.

Bioplastic characterization

Mechanical properties

The mechanical properties of the bioplastic specimens (20×100 mm^2) were evaluated using a tensile testing machine (AGS-X, Shimadzu, Japan) in accordance with ASTM D882. The initial gauge length was set at 50 mm, and the crosshead speed was maintained at 20 mm/min. Each formulation was tested in 5 replicates to ensure data reliability.

Fourier-Transform Infrared (FTIR) spectroscopy

Before drying for FTIR analysis, the specimens were rinsed with distilled water for 4 min to eliminate unreacted acid residues. FTIR spectrometer equipped with ATR accessory (Bruker, USA), utilizing 32 scans at a resolution of 4 cm^{-1} within the wavenumber range of 4,000 to 600 cm^{-1} to characterize the functional groups on the material surfaces.

Scanning electron microscope

Microstructural analysis of the surface and cross-sections of the synthesized biofilms was performed using an SEM (JEOL JSM5410 (JEOL Ltd., Tokyo, Japan). The biofilms were chopped into 5 Å ~ 1 mm^2 pieces, which were then placed on copper stubs. A 10 kV accelerating voltage was used to view samples coated with gold. For surface morphology, the images were taken at a magnification of Å ~ 10,000, and for their cross-section, at Å ~ 25,000.

Moisture Content (MC), Swelling Degree (SD), and Water Solubility (WS)

The bioplastic samples were cut into 3×3 cm^2 squares and initially weighed (M1). They were then dried in an oven at 100 °C for 4 h and reweighed (M2). After drying, the samples were immersed in a beaker containing 50 mL of distilled water at room temperature for 24 h. Undissolved bioplastics fragments were filtered out and weighed (M3) after gently removing excess surface water. Finally, the samples were dried in an oven at 105 ± 2 °C until a constant weight was achieved (M4). The moisture content (MC% %), swelling degree (SD% %), and water solubility (WS% %) were calculated based on Eqs. (3) - (5), respectively [24].

$$\mathrm{MC}\,\% = \frac{\mathrm{M1} - \mathrm{M2}}{\mathrm{M1}} \times 100 \quad (3)$$

$$\mathrm{SD}\% = \frac{\mathrm{M3} - \mathrm{M2}}{\mathrm{M2}} \times 100 \quad (4)$$

$$\mathrm{WS}\% = \frac{\mathrm{M2} - \mathrm{M4}}{\mathrm{M2}} \times 100 \quad (5)$$

Bioplastic thickness test

Bioplastic was measured using a digital micrometer (Syntek MIC7B) with an accuracy of 0.001 mm. The sample was measured at five points, and its thickness was determined by averaging the data.

Biodegradability test

Biodegradability was assessed using the burial method described by Wronska *et al.* [7], with some modifications. Firstly, the square-shaped bioplastic (3×3 cm^2) was weighed (W0) and then buried on a laboratory scale for 7 - 21 days (pH 5 and moisture 25% - 40%). At the determined time, the weight of the buried samples was measured (Wq), and the weight loss (WL) in % was calculated using Eq. (6).

$$\mathrm{WL}\,\% = \frac{\mathrm{Wo} - \mathrm{Wq}}{\mathrm{Wo}} \times 100 \quad (6)$$

Statistical analysis

Statistical analysis was performed using SPSS software (version 29, IBM Corp., Armonk, NY, USA). Data were expressed as mean ± standard deviation. One-way analysis of variance (ANOVA) followed by Duncan's multiple range test was used to evaluate the effect of citric acid concentration at a significance level of $p < 0.05$. The statistical interpretation in this study was primarily based on significance testing, while confidence intervals and effect size analyses were not included and should be considered in future studies to provide more comprehensive statistical validation.

Results and discussion

Chitosan characterization

BSFL pupae characterization

Chitosan is mainly derived from crustaceans, such as shrimp and crab. This study isolated chitosan from BSF pupae using a chemical extraction. **Table 1** presents a proximate analysis comparing BSF pupae with other chitosan sources. The results of the comparison between raw materials and chitosan are shown in **Figure 1**.

Table 1 The proximate analysis comparing BSF pupae and other chitosan sources.

Sample	Parameter					Ref
	Moisture (%)	Ash (%)	Protein (%)	Fat (%)	Carbohydrate (%)	
Pupae BSFL	4.69 ± 0.01	20.54 ± 0.32	39.77 ± 0.13	11.13 ± 0.24	23.86 ± 0.04	This study
Shrimp shells	N/A	23.8 ± 0.1	44.1 ± 1.0	1.29 ± 0.04	N/A	[27]
Red Shrimp	74.5 ± 0.7	2.0 ± 0.1	21.4 ± 0.2	0.1 ± 0.1	N/A	[28]

Chitosan yield

The chitosan yield from BSF pupae (**Figure 1**) was 7.64%. This study is similar to Siddiqui *et al.* [29], which shows that the chitin content of BSF varies from 8% to 24%, whereas the Rodriguez *et al.* [30] study shows a chitosan yield from BSFL cuticles ranging from 2% to 16%. However, this result is lower than the studies reported by El Feky *et al.* [26] (18% chitosan yield from *Aristeus antennatus* shells) and Abdulkarim *et al.* [31] (15.14% chitosan yield from mussel shells). This may be due to the defatting and deproteinization, which cause sample mass loss. Furthermore, defatting, deproteinization, and demineralization of pupae resulted in a mass loss of approximately 12.88%, 65.25%, and 41.19%, respectively. Additionally, mass losses reduced yield due to the removal of acetyl groups, protein, and lipids during extraction and washing. Furthermore, the sequence of the chitosan extraction stages also influences chitosan yield [30].



Figure 1 Sample BSF and Pupa's chitosan.

Degree of Deacetylation (DD) value of chitosan

In addition to yield, one indication of successful chitosan extraction is the degree of deacetylation (DD) value. According to Rodriguez *et al.* [30], a characteristic of chitosan is its entirely or partially deacetylated amine groups (> 50%), which explains its solubility in dilute acids and its bioactivity. In this study, the chitosan

produced had a DD of 84.80%. The % DD was determined by titration with methyl orange indicator, which estimates the number of free amine groups in chitosan. This value is quite high and meets the quality standards for commercial chitosan, which range from 70% - 95% [32]. A high DD indicates that the deacetylation process is optimal, with most acetyl groups in chitin successfully converted into amine groups. In addition, high DD is desirable when degradability is required [33,34]. Furthermore, it positively affects the functional properties of chitosan, including increased solubility in weak acid solutions, improved film-forming ability, and enhanced antimicrobial and biocompatibility.

Solubility of chitosan

The solubility of chitosan derived from pupae is approximately 50% or 5 g/L. This value is lower than the solubility of chitosan obtained from Aristeus antennatus shells (98.15%) [26] and commercial chitosan (99%) [35]. Chitosan solubility and degree of deacetylation (DD) are usually positively correlated. In contrast, the present study indicates an inverse relationship. This phenomenon is attributed to excessive protonation after deacetylation, which increases hydrogen bonding and leads to a more crystalline, dense chitosan structure. Such structural changes can inhibit solvent penetration and reduce solubility [36].

Cellulose characterization

This study used cellulose from OPEFB as a substrate filling for bioplastic production. Its addition serves as a reinforcing material, improving mechanical properties such as tensile strength, elastic modulus, and thermal stability. By reducing porosity and increasing homogeneity, cellulose further enhances film structure, making the bioplastic stronger and more durable. The results of cellulose from OPEFB after depigmentation are shown in **Figure 2**.

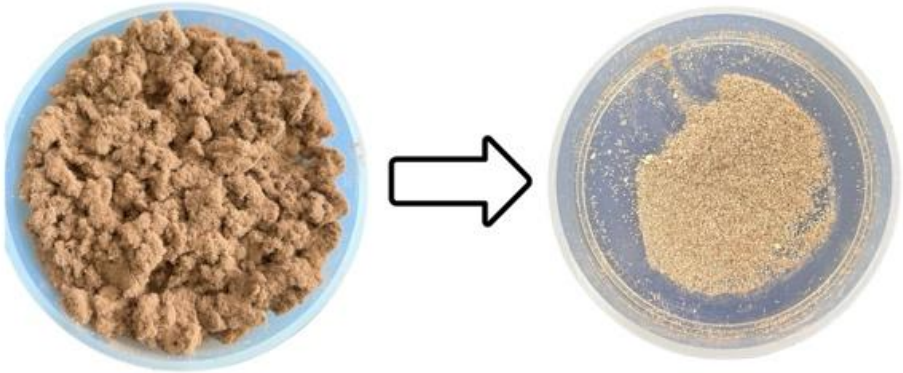


Figure 2 Cellulose from OPEFB after depigmentation.

Figure 3 presents the FTIR spectra of OPEFB cellulose. The absorption bands confirm the successful extraction of cellulose. The absorption peak at 3,334.43 cm^{-1} corresponds to the hydroxyl group, indicating intra- and intermolecular hydrogen bonding. Salim *et al.* [37] also reported that the 3,000 - 3,750 cm^{-1} region is associated with hydroxyl group activities. The band at 2,897.89 cm^{-1} is attributed to the aliphatic C–H stretching of methyl and methylene groups present in cellulose and hemicellulose. Fiore *et al.* [38] reported similar findings. The absorption band at 1,586.64 cm^{-1} is associated with water molecules bound to the cellulose structure. The bands at 1,425.49 cm^{-1} and 1,334.29 cm^{-1} correspond to the CH_2 and CH groups of cellulose, respectively. According to Kostryukov *et al.* [39], the identification of cellulose was carried out using the absorption band around 1,450 cm^{-1} (integrated over the range of 1,405 – 1,480 cm^{-1}), which primarily corresponds to the scissoring motion of methylene (–CH_2–) groups and the in-plane bending vibrations of hydroxyl (–OH) groups. The band at 1,159.44 cm^{-1} indicates the C–O–C group of the glycosidic bond, while the bands at 1,051.05 and 1,027.87 cm^{-1} are attributed to the C–O groups of secondary and primary alcohols. The peak at 896.06 cm^{-1} is characteristic of β-1,4-glycosidic stretching, typical of cellulose.

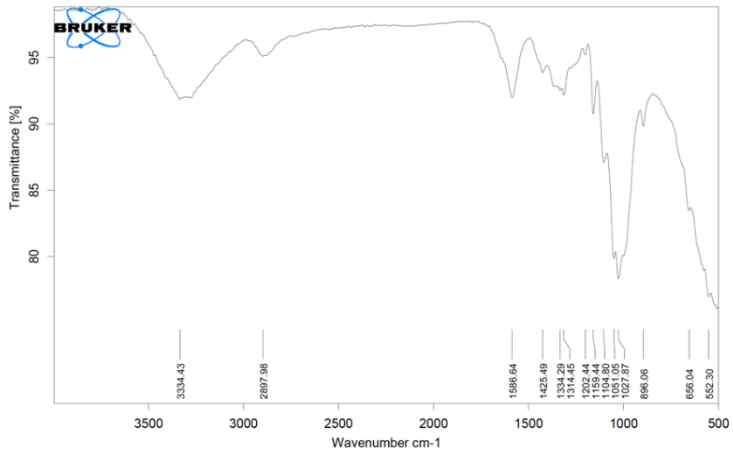


Figure 3 FTIR from OPEFB cellulose.

These findings are consistent with the XRD analysis shown in **Figure 4**, where the diffraction peaks at 2θ = 15° - 16°, 22°, and 34° correspond to the typical crystalline planes of cellulose I. The presence of these crystalline reflections confirms that the extracted cellulose retained its native crystalline structure. The relatively high crystallinity index (66%) is supported by the strong hydrogen-bonding interactions observed in the FTIR spectra, since hydrogen bonding contributes significantly to the formation and stabilization of crystalline regions in cellulose. The relatively high crystallinity index (66%) of the cellulose is expected to contribute positively to the structural reinforcement of the bioplastic matrix. Crystalline regions generally improve mechanical strength, thermal stability, and resistance to molecular mobility due to their ordered molecular arrangement and strong intermolecular hydrogen bonding. In the present study, the semi-crystalline structure of the cellulose likely contributed to the compact morphology observed in the composite films.

The FTIR and XRD results showed a strong correlation in confirming the structural characteristics of the cellulose. The broad hydroxyl absorption band observed in the FTIR spectra indicated extensive intra- and intermolecular hydrogen bonding, which contributed to the ordered arrangement of cellulose chains. This finding was supported by the XRD pattern, which exhibited characteristic cellulose I diffraction peaks and a relatively high crystallinity index. The presence of crystalline regions suggests that the hydrogen bonding interactions played an important role in stabilizing the semi-crystalline structure of the cellulose.

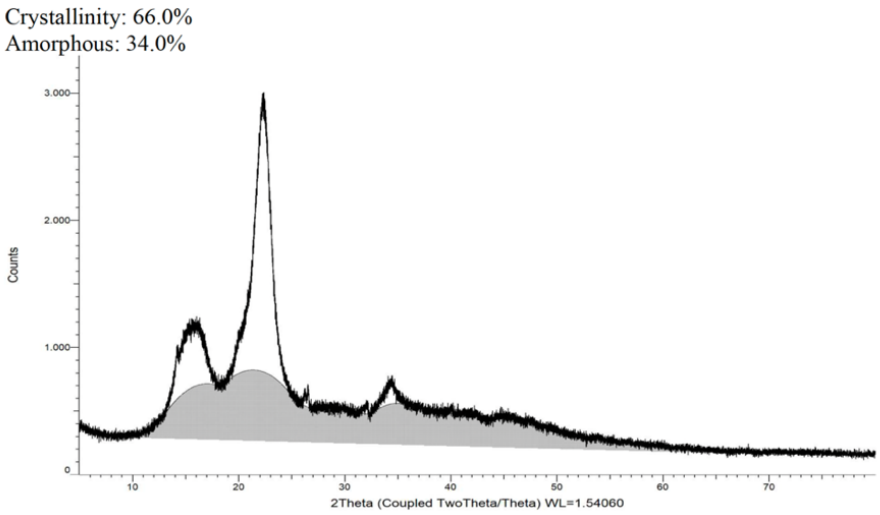


Figure 4 XRD from OPEFB cellulose.

Bioplastic characterization

Mechanical properties

Figure 5 shows the mechanical properties of the bioplastics. The tensile strength (TS) and elongation at break (EAB) of CS/C/S bioplastic were 0.13 MPa and 9.58%, respectively. An improvement trend was observed with the addition of CA, where the addition of 2.5 wt% CA resulted the highest TS of 0.64 MPa. This value remains lower than those reported for chitosan-based bioplastic prepared from commercial chitosan [24]. Previous study Ianniciello *et al.* [19], reported that films prepared from pure commercial chitosan exhibited a TS of 1.09 MPa, while films derived from bleached adult chitosan (BC-A), unbleached adult chitosan (UC-A), bleached larval chitosan (BC-L), and bleached pupal chitosan (BC-PE) showed lower TS values of 0.46, 0.63, 0.59, and 0.58 MPa, respectively. However, these values are considerably lower than those obtained in the present study, particularly for films prepared from bleached BSFL chitosan. These findings indicate that films prepared from BSFL chitosan exhibit relatively low TS. The relatively low TS of the BSF-derived chitosan bioplastics can be attributed to the intrinsic properties of the raw material, particularly its lower degree of deacetylation (DD) and molecular weight (MW) resulting from bleaching process. Bleaching of BSFL chitosan further reduces its mechanical performance, potentially due to a decrease in molecular weight [19]. In addition, chitosan extracted from BSF pupae exhibits a substantially lower MW (30.62 ± 0.27 kDa) than commercial crab-shell chitosan (~200 kDa) [17], which further limits film strength. Previous studies have consistently reported that higher MW and DD enhance mechanical properties by promoting stronger intermolecular interactions [18].

The addition of citric acid (CA) generally increased the tensile strength (TS) of the bioplastics, except at 7.5% CA, which may be associated with an imbalance between intermolecular interactions and matrix homogenity at low CA content. In contrast to TS, the elongation at break (EAB) exhibited an opposite trend, decreasing with increasing rigidity of the bioplastics, which is consistent with previous reports by Chen *et al.* [8]. The enhancement in TS can be attributed to the increased density of intermolecular hydrogen bonding within the bioplastic matrix induced by CA, which promotes stronger interactions between cellulose and chitosan (**Figure 5**). Enhanced hydrogen bonding has been reported to induce structural reorganization of polysaccharide chains, resulting in a more compact and homogeneous polymer network [25]. This densification restricts polymer chain mobility and improves interfacial adhesion between polymer components, enabling more efficient stress transfer under tensile loading and consequently increasing TS. Conversely, the reduction in EAB with increasing CA content is attributed to the formation of a physically crosslinked, hydrogen-bonded network that limits chain mobility and increases material rigidity [8]. These findings indicate that citric acid predominantly acts as a physical crosslinking agent, enhancing hydrogen bond density and stress transfer efficiency rather than forming covalent ester linkages. Compared to commercial chitosan-based bioplastics, the mechanical strength in this study remains lower. However, the addition of citric acid improved water resistance and intermolecular interactions within the bioplastic matrix. The stress–strain evaluation in this work was limited to tensile strength and elongation at break; therefore, more detailed mechanical analysis is recommended for future studies.

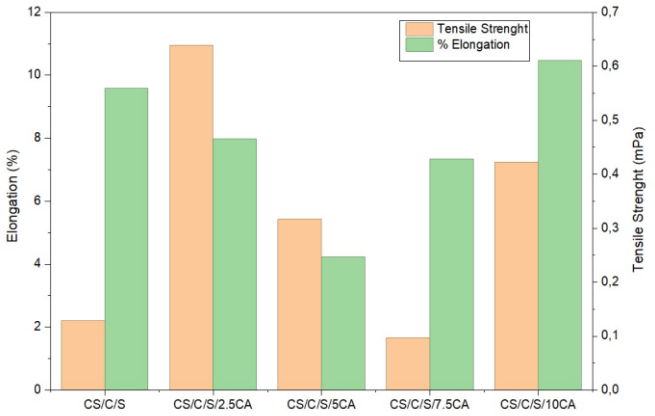


Figure 5 Tensile strength and elongation at break of bioplastic.

Physical properties

In this study, bioplastic was produced from pupae-derived chitosan combined with EFB-derived cellulose, using acetic acid. The results showed different visual characteristics for each treatment, as depicted in **Figure 6**. In general, the bioplastic had a flat and compact surface. The color of the bioplastic also tended to be a transparent yellow, influenced by the BSF chitosan.

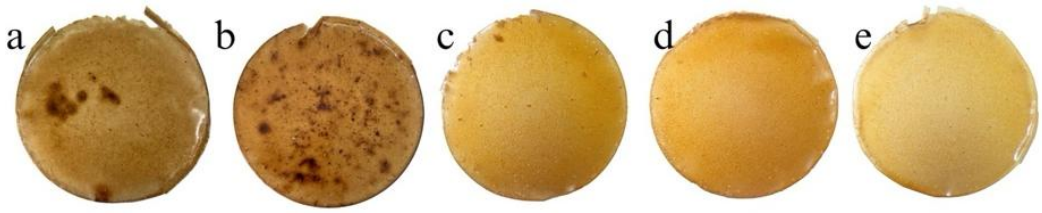


Figure 6 Bioplastic: (a) CS/C/S; (b) CS/C/S/2.5CA; (c) CS/C/S/5CA; (d) CS/C/S/7.5CA; (e) CS/C/S/10CA.

The bioplastics were physically analyzed, as shown in **Table 2**. The results showed that adding CA to CA/C/S bioplastics significantly affected moisture content (MC) and swelling degree (SD). However, there is no significant impact on water solubility (WS). MC was calculated to evaluate the ability of bioplastics to absorb water from the environment. As shown in **Table 2**, the MC value decreased significantly from 13.04% to 8.78% in the CS/C/S bioplastic when CA was added. A similar result was also shown in the SD. When CA was added, the SD significantly decreased from 75.07% to 33.675% in the CS/C/S bioplastic. Similar results were reported by Yao *et al.* [40] and Khadsai *et al.* [24]. MC and SD are highly sensitive to changes in surface properties and film microstructure, such as the number of free hydroxyl groups, and porosity. Adding CA adjusts the proportion between hydrophilic and hydrophobic groups, consequently impacting the film's capacity to absorb moisture and swell during soaking. Among the samples tested, CS/C/S/2.5CA exhibited the lowest MC and SD compared to CS/C/S/5CA, CS/C/S/7.5CA, and CS/C/S/10CA. This behavior can be attributed to the introduction of 2.5% citric acid, which promotes the formation of a physically crosslinked network through strong intermolecular hydrogen bonding between the carboxyl (–COOH) groups of citric acid and the hydroxyl (–OH) or amine ($–NH_2$) groups within the polymer matrix. The enhanced intermolecular interactions reduce the availability of hydrophilic functional groups and limit polymer chain mobility, thereby decreasing water uptake and swelling. As a result, a denser and more hydrophobic structure is formed [40]. It results in a significant reduction in MC and SD values compared to the control values. However, the WS of bioplastics increases with increasing CA concentration. This observation indicates that a portion of the CA does not undergo complete reaction, resulting in many free carboxylic (–COOH) groups. It contributes to the film's enhanced hydrophilic properties [10].

Table 2 Effect of CA on physical properties of bioplastics.

Bioplastic	Moisture Content (MC) (%)	Swelling Degree (SD) (%)	Water Solubility (WS) (%)	Thickness (mm)
CS/C/S	13.04[c]	75.07[b]	55.00[a]	0.294[a]
CS/C/S/2.5CA	8.78[a]	33.67[a]	33.70[a]	0.435[a]
CS/C/S/5CA	13.69[c]	39.78[a]	40.85[a]	0.298[a]
CS/C/S/7.5CA	11.64[b]	41.86[a]	44.22[a]	0.379[a]
CS/C/S/10CA	15.18[d]	44.76[a]	44.76[a]	0.341[a]

Data in the same column with different superscripts are significantly different ($p < 0.05$). The crosslinking was conducted with 0%, 2.5%, 5%, 7.5%, and 10%.

The WS of bioplastics is summarized in Table 2. Among the samples, CS/C/S/2.5CA shows the lowest WS at 33.70%. Notably, the water solubility of CS/C/S with 5% - 10% CA is lower than that of CS/S without CA. Similar findings were reported by Awadhiya *et al.* [41], who found that adding CA can effectively reduce water solubility. It implies reducing the number of hydrophilic hydroxyl groups and increasing the number of hydrophobic ester groups formed between chitosan, cellulose, and CA. However, as the concentration of CA increases, the solubility increases gradually. This condition indicates an incomplete chemical reaction between CA and the polymer chain. Most CA molecules form only weak interactions with hydroxyl or amine groups, which prevents the formation of ester bonds that enhance hydrophobicity, leading to more hydrophilic groups interacting with water molecules and reducing the water resistance of bioplastics [10,40]. Yao *et al.* [40] also identified a similar phenomenon. This finding highlight that the ratio of CA to reactive groups in the polymer is crucial for achieving a balanced set of physical properties and optimal water resistance.

Table 2 demonstrates that the bioplastic produced has a thickness ranging from 0.294 to 0.435 mm. Thickness is an important factor that indicates the quality and uniformity of the bioplastic [4]. However, in this study, the addition of CA did not significantly influence the thickness of the bioplastic. The small amounts of CA incorporated into the bioplastic did not significantly affect the total viscosity or the distribution of solids in solution, indicating that the film's physical volume remained relatively constant across treatments. The observed variation in bioplastic thickness can be explained by the relatively low DD and MW of BSFL pupal chitosan. Low DD limits chitosan solubility in dilute acetic acid, leading to a reduced effective polymer concentration in the casting solution [17,42]. As a result, thinner films were formed during solvent evaporation [17], which is consistent with previous reports linking chitosan solubility and molecular characteristics to film thickness and morphology [41].

FTIR spectra

FTIR analysis is conducted to identify functional chemical groups and molecular interactions involved in bioplastic. As shown in **Figure 7**, the incorporation of citric acid (CA) did not result in the appearance of a distinct ester carbonyl band in the 1,720 - 1,750 cm^{-1} region, which is typically associated with strong covalent esterification [10,24]. This indicates that extensive ester bond formation was not achieved. Instead, subtle spectral changes were observed in the 1,050 - 1,150 cm^{-1} region, attributed to C–O stretching vibrations, which may indicate changes in intermolecular interactions within the polymer matrix. In addition, a slight attenuation of the broad O–H stretching band (3,200 - 3,600 cm^{-1}) was observed with increasing CA content, suggesting enhanced hydrogen bonding interactions between citric acid and the polysaccharide chains. The shift and attenuation of the –OH band suggest the formation of hydrogen bonding between citric acid and the biopolymer matrix, suggesting improved intermolecular compatibility within the polymer matrix. These strengthened intermolecular interactions may contribute to the improved physical and mechanical properties of the bioplastic.

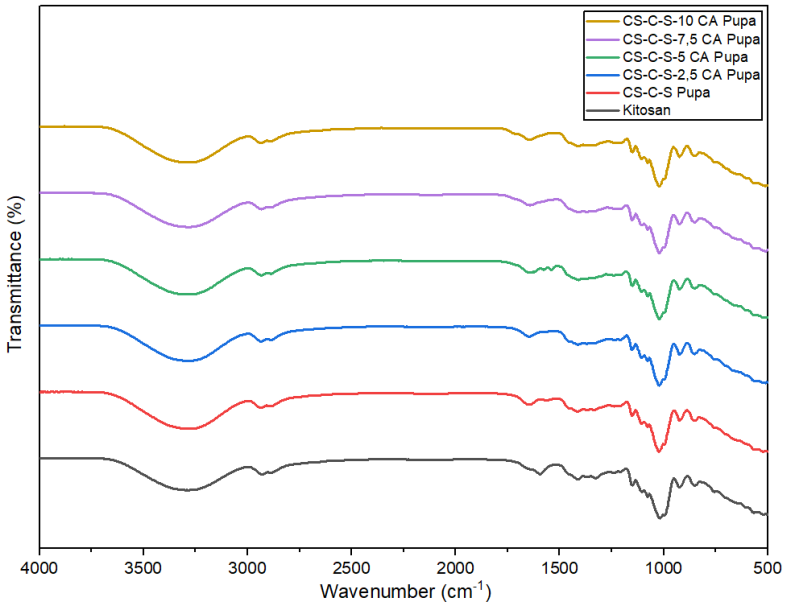


Figure 7 FTIR spectra of bioplastic made of chitosan-cellulose-starch (CS/C/S) with citric acid (CA).

The reduction in moisture content and swelling degree observed in the CS/C/S/2.5CA formulation may be associated with the enhanced intermolecular interactions and reduced availability of free hydrophilic groups within the matrix. However, the relatively low tensile strength and moderate elongation values indicate that the interactions formed were predominantly physical rather than strong covalent crosslinking. Therefore, citric acid likely functioned mainly as a physical crosslinking agent through hydrogen bonding, contributing primarily to improved water resistance and structural compactness rather than substantial mechanical reinforcement.

Bioplastic morphology

To investigate the effects of citric acid on surface morphology and matrix homogeneity, Scanning Electron Microscopy (SEM) analysis was conducted; the results are presented in **Figure 8**. The micrographs of CS/C/S bioplastics show a smooth surface devoid of pores, indicating high compatibility between the constituent materials. This observation aligns with the findings of Wu *et al.* [10], demonstrating significant molecular miscibility between chitosan and starch. However, significant variations were seen with different concentrations of citric acid (CA). The addition of 2.5% and 5% CA results in a denser surface morphology, characterized by the absence of cracks, suggesting strong intermolecular interactions within the bioplastic matrix. In this study, CS/C/S/2.5CA film exhibited a denser and more homogeneous surface structure compared to the other formulations. The reduced presence of pores and voids suggests improved intermolecular interactions within the polymer matrix, likely promoted by hydrogen bonding between citric acid and the biopolymer components. This compact morphology is consistent with the improved physical and mechanical properties observed in the film. The denser structure likely facilitated more effective stress transfer throughout the matrix, resulting in higher tensile strength compared to the other treatments. In addition, the reduced free volume and lower porosity may have limited water penetration into the film matrix, contributing to the lower moisture content and swelling degree observed in the CS/C/S/2.5CA sample.

In contrast, the incorporation of 7.5% and 10% citric acid resulted in a rough and inhomogeneous surface morphology characterized by the presence of aggregates or lumps. This behavior may be attributed to excessive citric acid content, which promotes uneven intermolecular interactions and localized network densification, leading to polymer phase aggregation and, consequently, reduced flexibility and homogeneity. This condition may increase hydrophilicity and reduce structural integrity, leading to lower tensile strength and increased water solubility. Wu *et al.* [10] confirmed this finding, similarly observing that the addition of 20% CA yielded a bioplastic with a markedly rougher surface.

Such findings underscore the critical role of citric acid concentration in influencing the structural and functional properties of bioplastics synthesized from chitosan and starch.

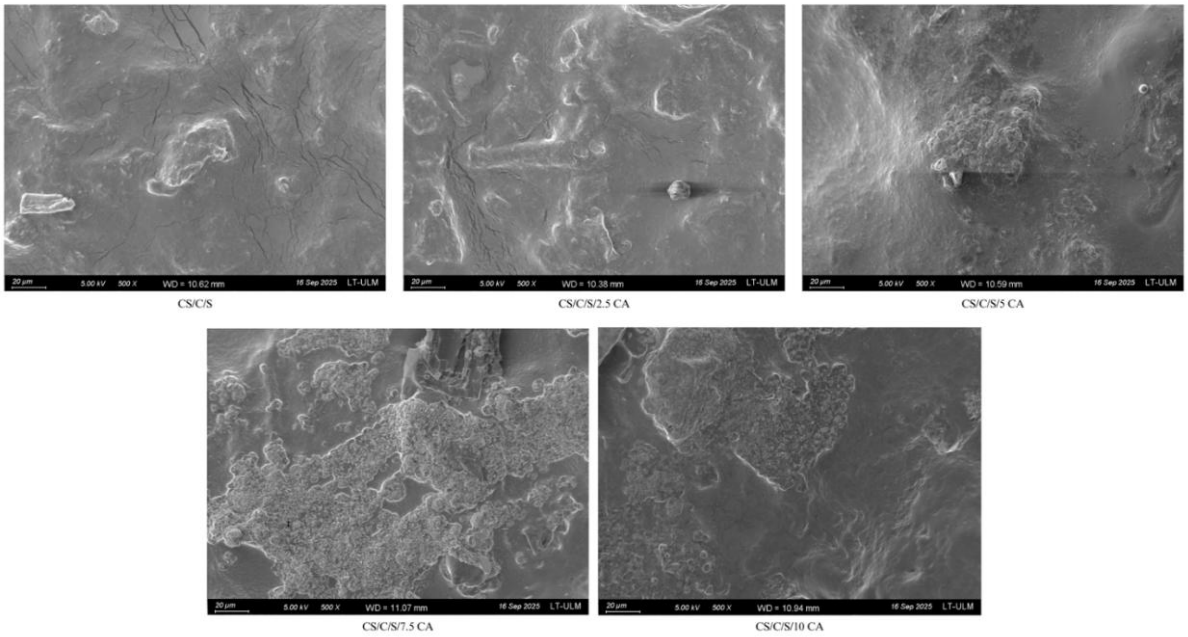


Figure 8 SEM micrograph Bioplastic made of chitosan-cellulose-starch (CS/C/S) with citric acid (CA).

Bioplastic biodegradability

Biodegradation testing is essential to assess the rate of bioplastic decomposition in the environment. **Figure 9** shows that bioplastics containing CA exhibited a slower weight loss rate compared to the CS/C/S control, indicating enhanced resistance to degradation. This behavior suggests the formation of a more compact polymer network promoted by intermolecular interactions between CA and the CS/C/S matrix. The reduced degradation rate is mainly attributed to strong intermolecular interactions, such as hydrogen bonding between the carboxyl (–COOH) groups of CA and the hydroxyl (–OH) and amino ($–NH_2$) groups of chitosan and cellulose, which result in a denser and less water-permeable structure. This compact network limits water penetration and microbial accessibility, thereby slowing down the degradation process. Similar observations have been reported by Awadhiya *et al.* [41].

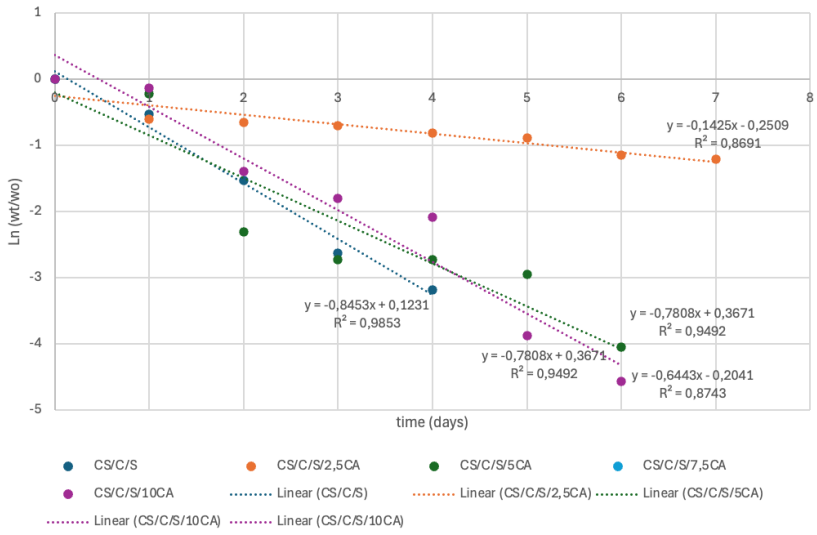


Figure 9 Kinetics of CS/C/S bioplastic films with different citric acid concentrations.

Figure 9 demonstrates that the CS/C/S/2.5CA bioplastic exhibited the lowest degradation rate constant ($k = 0.1425$ day^{-1}), indicating the slowest degradation behavior and the highest structural stability among all formulations. This finding is consistent with the SEM observations, which revealed that the CS/C/S/2.5CA film possessed a denser and more homogeneous morphology compared to the other treatments. In addition, this formulation exhibited improved physical and mechanical properties. Furthermore, the incorporation of 2.5% citric acid promoted enhanced hydrogen-bonding interactions within the polymer matrix, contributing to the formation of a more compact and stable bioplastic structure.

Bioplastics formulated with high concentrations of citric acid (CA) tended to degrade more rapidly by day 7 compared to the formulation containing 2.5% CA. The presence of citric acid promoted the formation of a more compact polymer network (**Figure 10**), which restricted water diffusion and reduced the accessibility of polymer chains to hydrolytic and biological agents. This structural densification limited swelling and slowed hydrolytic degradation, resulting in a lower biodegradation rate compared to bioplastics with a less compact polymer structure. The reduced degradation behavior is attributed to enhanced intermolecular interactions induced by citric acid, which hinder water penetration and microbial interaction with the polymer matrix, as also reported by Awadhiya *et al.* [41]. However, an excess concentration of CA enhances the hydrophilicity and porosity of the polymer matrix, leading to the formation of microscopic holes that facilitate increased porosity and water diffusion within the material. Although the findings indicate a decrease in weight loss, the bioplastic's biodegradability is controlled by the presence of hydroxyl groups (-OH), which contribute to its susceptibility to degradation [5,43]. This is further evidenced by visual color, weight, and morphology changes, as illustrated in **Figure 10**. However, although hydrogen bonding enhances the material's resistance to initial degradation, it does not completely inhibit microbial activity responsible for bioplastic decomposition.

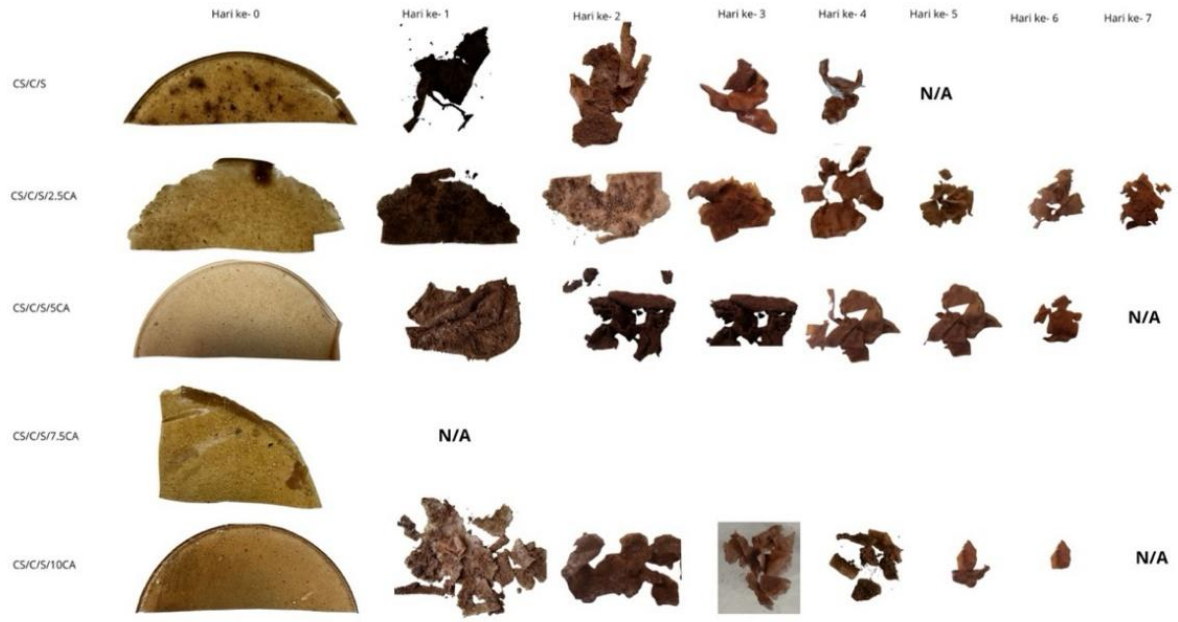


Figure 10 Result of biodegradation of bioplastic made of chitosan-cellulose-starch (CS/C/S) with citric acid (CA).

Conclusions

The incorporation of citric acid (CA) significantly affected the mechanical and physical properties, moisture content, swelling degree, water solubility, and biodegradability of the CS/C/S bioplastics. Compared with the films prepared without CA, the CA-containing bioplastics exhibited improved tensile strength and reduced moisture sensitivity. The tensile strength (TS) increased with increasing CA concentration, while the elongation at break (EAB) showed an opposite trend, indicating reduced flexibility of the films. This behavior may be attributed to enhanced intermolecular hydrogen bonding between the carboxyl (–COOH) groups of CA and the hydroxyl (–OH) and amino ($–NH_2$) groups of chitosan and cellulose, leading to the formation of a more compact and cohesive polymer network. Among all formulations, the CS/C/S film containing 2.5 wt% CA exhibited the most balanced overall performance, showing optimal mechanical properties alongside reduced moisture content (8.78%), swelling degree (33.67%), water solubility (33.67%) and the lowest degradation rate constant (($k = 0.1425\ day^{-1}$). The lower (k) value indicates slower degradation behavior and improved structural stability compared with the other formulations. These findings were consistent with the SEM observations, which revealed a denser and more homogeneous morphology for the CS/C/S/2.5CA film. Furthermore, FTIR analysis suggested enhanced intermolecular hydrogen-bonding interactions within the polymer matrix, which likely contributed to the improved structural compactness, reduced water penetration, and slower degradation rate of the bioplastic film. Nevertheless, the mechanical strength of the developed bioplastics remained relatively low compared to previously reported chitosan-based bioplastics derived from crustacean sources. Therefore, the present findings should be interpreted within the scope of the current formulation and processing conditions. In addition, durability-related properties such as long-term stability, barrier performance, thermal aging resistance, and storage stability were not evaluated in this study. Although FTIR analysis did not reveal a distinct ester carbonyl peak in the 1,720 - 1,750 cm^{-1} region, indicating that extensive covalent esterification was not achieved, future studies may focus on optimizing the crosslinking process to promote stronger covalent interactions within the polymer matrix. Approaches such as extending thermal treatment duration, controlling pH under mildly acidic conditions, or employing dehydration catalysts and coupling agents may facilitate thermally activated esterification between citric acid and polysaccharides. Furthermore, advanced characterization techniques, including solid-state NMR and more sensitive spectroscopic analyses, are recommended to provide more conclusive evidence of ester bond formation and crosslinking mechanisms.

Acknowledgements

This research received valuable support from the Ministry of Research and Technology, Indonesia through the DRTPM grant, as part of the 2025 Fundamental Bima scheme (DIPA No: SP DIPA-139.04.1.693320/2025).

Declaration of Generative AI in Scientific Writing

The authors also acknowledge the use of ChatGPT (OpenAI, USA) and Grammarly (Grammarly Inc., USA) to improve the English language and clarity of the manuscript. All text was carefully reviewed and verified by the authors to ensure accuracy and integrity of the content.

CRediT Author Statement

Novianti Adi Rohmanna: conceptualization, Methodology, Data Curation, Writing-Original Draft, Writing-Review and Editing; **Utami Irawati**: Methodology, Data Curation, Validation, Writing-Review and Editing; **Hemy Sriana**: Project Administration, Methodology; **Muhammad Rido**: Resources; **Fidel Castro Haholongan Purba**: Investigation, Methodology; **Muhammad Rasyad**: Investigation, Methodology.

References

[1] BR Nogueira, BP Backx and T Delazare. Starch, pectin and chitosan-based bioplastics with silver nanoparticles: An eco-friendly alternative for the food industry. *Sustainable Chemistry for the Environment* 2025; **10**, 100246.

[2] SX Tan, HC Ong, A Andriyana, S Lim, YL Pang, F Kusumo and GC Ngoh. Characterization and parametric study on mechanical properties

enhancement in biodegradable chitosan-reinforced starch-based bioplastic film. *Polymers* 2022; **14(2)**, 278.

[3] J Pires, CDD Paula, VGL Souza, AL Fernando and I Coelhoso. Understanding the barrier and mechanical behavior of different nanofillers in chitosan films for food packaging. *Polymers* 2021; **13(5)**, 721.

[4] R Ratna, M Mutia, D Darwin, AA Munawar, F Fitriani and L Handayani. Utilization of tofu liquid waste for the manufacture of bioplastic food packaging. *Case Studies in Chemical and Environmental Engineering* 2024; **10**, 100830.

[5] H Hernando, Marpongahtun, E Julianti, A Nuryawan, SA Amaturrahim, AFR Piliang, MR Yanhar, R Goei, N Soykeabkaew, AMA Saputra and S Gea. Impact of glycerol on oil palm trunk starch bioplastics enhanced with citric-acid epoxidized palm oil oligomers. *Case Studies in Chemical and Environmental Engineering* 2024; **10**, 100839.

[6] D Nuvoli, G Montevecchi, F Lovato, F Masino, MVD Borght, M Messori and A Antonelli. Protein films from black soldier fly (*Hermetia illucens*, Diptera: Stratiomyidae) prepupae: Effect of protein solubility and mild crosslinking. *Journal of the Science of Food and Agriculture* 2021; **101(11)**, 4506-4513.

[7] N Wrońska, N Katir, M Nowak-Lange, A El-Kadib and K Lisowska. Biodegradable chitosan-based films as an alternative to plastic packaging. *Foods* 2023; **12(18)**, 3519.

[8] WC Chen, SNMS Mohd Judah, SK Ghazali, DI Munthoub, H Alias and Z Mohamad. The effects of citric acid on thermal and mechanical properties of crosslinked starch film. *Chemical Engineering Transactions* 2021; **83**, 199-204.

[9] J Yang, S Xu, W Wang, X Ran, YC Ching, X Sui, Y Wei, R Wang and NM Al-Hada. Preparation and characterization of bioplastics from silylated cassava starch and epoxidized soybean oils. *Carbohydrate Polymers* 2023; **300**, 120253.

[10] H Wu, Y Lei, J Lu, R Zhu, D Xiao, C Jiao, R Xia, Z Zhang, G Shen, Y Liu, S Li and M Li. Effect of citric acid induced crosslinking on the structure and properties of potato starch/chitosan composite films. *Food Hydrocolloids* 2019; **97**, 105208.

[11] A Franco, C Scieuzo, R Salvia, AM Petrone, E Tafi, A Moretta, E Schmitt and P Falabella. Lipids from *Hermetia illucens*, an innovative and sustainable source. *Sustainability* 2021; **13(18)**, 10198.

[12] M Kalová and M Borkovcová. Voracious larvae Hermetia illucens and treatment of selected types of biodegradable waste. *Acta Universitatis Agriculturae et Silviculturae Mendelianae Brunensis* 2013; **61(1)**, 77-83.

[13] A Xiong, L Ruan, K Ye, Z Huang and C Yu. Extraction of chitin from black soldier fly (*Hermetia illucens*) and its puparium by using biological treatment. *Life* 2023; **13(7)**, 1424.

[14] R Rachmawaty, S Sahribulan, SE Putri and WF Arisma. Formation of chitosan from black soldier fly (Hermetia illucens) pupae using microwaves radiation energy. *Jurnal Aisyah: Jurnal Ilmu Kesehatan* 2023; **8(2)**, 1173-1180.

[15] RK Dewi, S Oktawati, A Gani, E Suhartono, N Hamrun, NA Rohmanna, S Riezqy and G Sugiarto. Synthesis, characterization, and *in silico* nanochitosan of pupa black soldier fly (*Hermetia illucens*) as bone graft material for bone remodeling post tooth extraction. *Journal of Chemical Health Risks* 2023; **13(4)**, 2370-2377.

[16] R Sulaeman, RRZDW Putri, R Damayanti, F Fauzan, MR Hadiyan and Y Maharani. Characterization of eco-friendly straw based on chitosan from pupae exuviae of black soldier fly (*Hermetia illucens*). *AgriHealth: Journal of Agri-Food, Nutrition and Public Health* 2024; **5(2)**, 92-100.

[17] A Simon, R Pramitasari, DSB Anugrah and DE Waturangi. Development of intelligent packaging films utilising chitosan derived from black soldier fly exuviae and anthocyanin from red dragon fruit peel for monitoring banana ripeness. *International Journal of Biological Macromolecules* 2025; **319**, 145610.

[18] S Affes, I Aranaz, N Acosta, Á Heras, M Nasri and H Maalej. Chitosan derivatives-based films as pH-sensitive drug delivery systems with enhanced antioxidant and antibacterial properties. *International Journal of Biological Macromolecules* 2021; **182**, 730-742.

[19] D Ianniciello, AP Montosa, RDM Barbosa, FG Villén, R Salvia, C Scieuzo, C Viseras and P Falabella. Development of chitosan-clay nanocomposite films from Hermetia illucens: Analysis of chemical, physical, and mechanical properties. *International Journal of Biological Macromolecules* 2025; **311**, 143496.

[20] E Marinho. Cellulose: A comprehensive review of its properties and applications. *Sustainable Chemistry for the Environment* 2025; **11**, 100283.

[21] EA Agustiany, DS Nawawi, AD Martino, FP Sari and W Fatriasari. Lignin-chitosan-based bioplastics from oil palm empty fruit bunches for seed coating. *Biocatalysis and Agricultural Biotechnology* 2024; **62**, 103435.

[22] M Nurdin, H Abimanyu, H Putriani, LOMI Setiawan, M Maulidiyah, D Wibowo, A Ansharullah, M Natsir, LOA Salim, Z Arham and F Mustapa. Optimization of OPEFB lignocellulose transformation process through ionic liquid [TEA][HSO_4] based pretreatment. *Scientific Reports* 2021; **11(1)**, 11338.

[23] N Sharmin, JT Rosnes, L Prabhu, U Böcker and M Sivertsvik. Effect of citric acid cross linking on the mechanical, rheological and barrier properties of chitosan. *Molecules* 2022; **27(16)**, 5118.

[24] S Khadsai, R Janmanee, P Sam-Ang, Y Nuanchawee, W Rakitikul, W Mankhong, W Likittrakulwong and P Ninjiaranai. Influence of crosslinking concentration on the properties of biodegradable modified cassava starch-based films for packaging applications. *Polymers* 2024; **16(12)**, 1647.

[25] K Miller, CL Reichert, M Schmid and M Loeffler. Impact of citric acid on the structure, barrier, and tensile properties of esterified/cross-linked potato peel-based films and coatings. *Polymers* 2024; **16(24)**, 3506.

[26] AR El-Feky, M Ismaiel, M Yılmaz, FM Madkour, A El-Nemr and HA Ibrahim. Biodegradable plastic formulated from chitosan of *Aristeus antennatus* shells with castor oil as a plasticizer agent and starch as a filling substrate. *Scientific Reports* 2024; **14(1)**, 11161.

[27] C Pedrazzani, L Righi, F Vescovi, L Maistrello and A Caligiani. Black soldier fly as a new chitin source: Extraction, purification and molecular/structural characterization. *LWT* 2024; **191**, 115618.

[28] R Rosa and ML Nunes. Nutritional quality of red shrimp, *Aristeus antennatus* (Risso), pink shrimp, *Parapenaeus longirostris* (Lucas), and Norway lobster, *Nephrops norvegicus* (Linnaeus). *Journal of the Science of Food and Agriculture* 2004; **84(1)**, 89-94.

[29] SA Siddiqui, L van Greunen, A Zeiri, B Yudhistira, A Ahmad and M Monnye. The potential of chitin and chitosan from dead black soldier fly (BSF) (*Hermetia illucens*) for biodegradable packaging material - A critical review. *Process Safety and Environmental Protection* 2024; **189**, 1342-1367.

[30] CE Rodríguez, V Zaremska, T Klammsteiner, I Kampatsikas, N Münstermann, O Weichold and S Gruber. Chitosan obtained from black soldier fly larval cuticles expands the value chain and is effective as a biocontrol agent to combat plant pathogens. *Carbohydrate Polymers* 2025; **349**, 123023.

[31] A Abdulkarim, MT Isa, S Abdulsalam, AJ Muhammad and AO Ameh. Extraction and characterisation of chitin and chitosan from mussel shell. *Extraction* 2013; **3(2)**, 108-114.

[32] M Rinaudo. Chitin and chitosan: Properties and applications. *Progress in Polymer Science* 2006; **31(7)**, 603-632.

[33] J Dutta. A facile approach for the determination of degree of deacetylation of chitosan using acid-base titration. *Heliyon* 2022; **8(7)**, e09924.

[34] A Tapia, R Seña, H Zambrano and V Paredes. Extraction and characterization of chitosan obtained from shells of crab (*Callinectes bocourti* and *Callinectes sapidus*). *International Journal of Biological Macromolecules* 2025; **320**, 145963.

[35] MS Hossain and A Iqbal. Production and characterization of chitosan from shrimp waste. *Journal of the Bangladesh Agricultural University* 2014; **12(1)**, 153-160.

[36] I Aranaz, AR Alcántara, MC Civera, C Arias, B Elorza, A Heras Caballero and N Acosta. Chitosan: An overview of its properties and applications. *Polymers* 2021; **13(19)**, 3256.

[37] R Md Salim, J Asik and MS Sarjadi. Chemical functional groups of extractives, cellulose and

lignin extracted from native *Leucaena leucocephala* bark. *Wood Science and Technology* 2021; **55(2)**, 295-313.

[38] V Fiore, T Scalici and A Valenza. Characterization of a new natural fiber from *Arundo donax* L. as potential reinforcement of polymer composites. *Carbohydrate Polymers* 2014; **106**, 77-83.

[39] SG Kostryukov, HB Matyakubov, YY Masterova, AS Kozlov, MK Pryanichnikova, AA Pynenkov and NA Khluchina. Determination of lignin, cellulose, and hemicellulose in plant materials by FTIR spectroscopy. *Journal of Analytical Chemistry* 2023; **78(6)**, 718-727.

[40] S Yao, BJ Wang and YM Weng. Preparation and characterization of mung bean starch edible films using citric acid as cross-linking agent. *Food Packaging and Shelf Life* 2022; **32**, 100845.

[41] A Awadhiya, D Kumar and V Verma. Crosslinking of agarose bioplastic using citric acid. *Carbohydrate Polymers* 2016; **151**, 60-67.

[42] Y Li, W Yokoyama, J Wu, J Ma and F Zhong. Properties of edible films based on pullulan–chitosan blended film-forming solutions at different pH. *RSC Advances* 2015; **5(128)**, 105844-105850.

[43] RC Nissa, AK Fikriyyah, AHD Abdullah and S Pudjiraharti. Preliminary study of biodegradability of starch-based bioplastics using ASTM G21-70, dip-hanging, and Soil Burial Test methods. *IOP Conference Series: Earth and Environmental Science* 2019; **277(1)**, 012007.